Food & Function

Filamentous fungal Pellet as a novel and sustainable encapsulation matrix for exogeneous bioactive compounds

SCHOLARONE™
Manuscripts

Filamentous fungal Pellet as a novel and sustainable encapsulation matrix for exogeneous bioactive compounds

Yixing Lu[1], Minami Ogawa[1], Jaime Moreno García[2], Nitin Nitin[1,3]*

Abstract

Edible filamentous fungi (FF) are considered a sustainable food material given its rich nutrient profile and low carbon and water footprints during production. The current study evaluated FF biomass as a natural encapsulation system for exogeneous bioactive compounds and as a model system to investigate the complex food matrix-micronutrient interactions during *in vitro* digestion. Our objective was to compare the fungal pellet, as a multicellular encapsulation system, with single yeast cell-based carriers in terms of loading and release of curcumin, a model compound. The results suggest that the curcumin encapsulation efficiency was similar in single yeast cells and fungal hyphae cells. A vacuum treatment used to facilitate infusion of curcumin into yeast or fungal cells also enabled rapid internalization of yeast cells into the fungal pellet matrix. Compared to the single-cell encapsulation system, the multicellular systems modified the release kinetics of curcumin during *in vitro* digestion by eliminating the initial rapid release and reducing the overall release rate of curcumin in the small intestinal phase. These results provide a deeper understanding on the effect of natural edible structures on the bioaccessibility of micronutrients, and demonstrate the potential of using FF biomass as functional food materials.

[1] *Department of Food Science and Technology, University of California-Davis, Davis, CA 95616, USA.*
[2] *Department of Agricultural Chemistry, Edaphology and Microbiology, University of Córdoba, 14014 Córdoba, Spain*
[3] *Department of Biological and Agricultural Engineering, University of California-Davis, Davis, CA 95616, USA.*

1. Introduction

Encapsulation is a widely used process in developing food ingredient formulations to improve the stability and controlled release of vital ingredients, including antioxidants, vitamins, bioactive peptides, flavors, aromas etc. [1–3] It often requires isolation and extraction of ingredients from food systems, as well as high energy processing technologies to generate colloidal particles with sub-micron to sub-millimeter scale sizes so that these ingredients can be incorporated in food formulations to achieve their desired functionality. Moreover, many of these encapsulation systems require the addition of exogenous preservatives to maintain the stability of encapsulated ingredients. In contrast to these engineered encapsulation systems, cell-based micro-carriers such as yeast cells have emerged as a sustainable encapsulation approach. The micron-scale sized yeast cells can be utilized as natural encapsulants without extensive fabrication, eliminating the need for extraction and purification of ingredients and reducing the energy input required to construct the colloidal delivery systems. Furthermore, many previous studies have reported that the yeast cells could enhance the oxidative and thermal stability [4–6] of the encapsulated molecules during storage compared to colloidal carriers such as emulsions.

Cell-based encapsulation concept also enables a unique approach to develop multicellular encapsulation systems. These multicellular encapsulation systems could enable controlled release and improved stability of encapsulated bioactives. In addition, these multicellular encapsulation systems can also be an effective model system for evaluating the food matrix effect on the release of micronutrients and encapsulated bioactives from encapsulation ingredients or food systems. Different release profiles of bioactives achieved based on the endogenous properties of the food matrix or design of the encapsulation systems can be beneficial for influencing the availability and functionality of bioactives along the GI tract, including the colon [7]. With this

overall motivation, we had engineered a 3D assembly of yeast cell-based micro-carriers in our previous study and compared the release profile of the bioactive compound from such cellular assemblies to that from single cells [8] during the simulated sequential digestion, i.e., combining both the gastric and small intestinal digestion phases. The results revealed that although the cell clustering could modify the release kinetics of the compound during digestion, this modification of a release rate was limited for a short term, i.e., the first 30 minutes of intestinal digestion. Moreover, the approach developed in this previous study required significant modifications of yeast cells with biopolymers to enable the formation of a multicellular encapsulation system. Thus, there is a need for a scalable approach to develop sustainable multicellular encapsulation systems without significant modifications for diverse applications in food systems.

In this study we developed a natural multicellular encapsulation system using filamentous fungal pellet to address the need for enhancing the sustainability of food ingredient technologies and to investigate the structural/matrix effect of cell-based encapsulation systems on the bioaccessibility of micronutrients. Filamentous fungus (FF) can grow on a variety of substrates [9–11], including food processing by-products and wastes, making the fungal biomass an affordable and sustainable material with low water and carbon footprints [12]. During submerged fermentation of FF, distinct fungal morphologies could be observed based on the selected fungal microorganisms and culturing conditions[13]. Fungal pellet (FP) is a dense, spherical aggregate of intertwining fungal hyphae that could be spontaneously formed by several FF species [14], such as *Aspergillus spp.*, *Penicillium spp.* etc. [15,16], under submerged, shaking culture conditions. FP has been used as a supporting biomaterial for immobilization of other microorganisms. For example, immobilization of yeast for winemaking [17], of microalgae and bacteria for wastewater treatment [18,19] and biofuel production [20,21], etc. Recently, FF *Aspergillus oryzae* has been shown to be a

good supporting material for growth of both yeast and animal cells [22]. Yeast biocapsule - the co-attachment of *Saccharomyces cerevisiae* and the FF *Penicillium chrysogenum* , is a well-studied system, especially for the applications of alcoholic fermentation, such as production of wine, beer, and bioethanol [23–26]. FP and yeast-FF biocapsule served as perfect multicellular model systems to study the matrix effect of these encapsulation systems on the release of encapsulated bioactives.

The two major objectives of the study were to 1) evaluate FF biomass as a natural multicellular encapsulation system for exogenous bioactive compounds, and 2) investigate the matrix effect endowed by the natural structure of the multicellular fungal pellet on the bioaccessibility of the encapsulated bioactive compound, and elucidate the potential factors contributing to this matrix effect. In the current study, *Saccharomyces cerevisiae* G1 strain was chosen as the model single-cell encapsulant because of its established ability to be immobilized onto fungal pellet formed by *P. chrysogenum* H3 [27]. Two multicellular encapsulation systems: the fungal pellet (FP) itself and yeast cells immobilized in FP were evaluated for their encapsulation yield of a model bioactive - curcumin during encapsulation and release during *in vitro* digestion. These results of multicellular encapsulation systems were compared to the single-cell system using the *S. cerevisiae* G1 cells as the microcarriers. The FF biomass has been identified as a good source of alternative protein since it can meet the basic nutritional requirements [28]. The method used in the current study provided a cost-effective way to encapsulate exogeneous bioactive compounds into the FF biomass, which further enhance its nutritional values. Moreover, with a better understanding on the complex matrix-micronutrient interaction within this natural multicellular system, we can further potentiate FF biomass as a functional food material.

2. Materials and methods

2.1. Materials

Curcumin derived from *Curcuma longa* (turmeric) [≥ 65%, HPLC], methanol, bile salts (cholic acid- deoxycholic acid sodium salt mixture), calcium chloride, potassium phosphate monobasic, ammonium phosphate, Calcofluor white, and Nile red were purchased from Sigma-Aldrich (St. Louis, MO). Sodium hydroxide, hydrochloric acid, sodium chloride, potassium chloride, magnesium chloride, sodium phosphate monobasic, yeast extract, peptone, and dextrose anhydrous were purchased from Fisher Scientific (Pittsburgh, PA). Absolute ethanol was purchased from Koptec (King of Prussia, PA). Corn meal agar was purchased from Neogene (Santa Clara, CA). Yeast nitrogen base without amino acids was purchased from BD (Franklin Lakes, NJ). D-Gluconic acid, 50% aqueous solution was purchased from Spectrum Chemicals (New Brunswick, NJ). The enzymes pepsin from porcine gastric mucosa (1064 units/mg protein) and pancreatin from porcine pancreas (4x USP) were purchased from Sigma-Aldrich (St. Louis, MO).

2.2. Microorganisms and growth media

Saccharomyces cerevisiae G1 *(MYA-2451)* and the filamentous fungus strain *Penicillium chrysogenum* H3 (UCDFST 22-448) were provided by the Department of Microbiology, University of Cordoba, Spain, and were used for the development of the single-cell and multicellular encapsulation model systems. *S. cerevisiae* G1 was grown in YPD broth (1 wt./vol.% yeast extract, 2 wt./vol.% peptone, and 2 wt./vol.% glucose) in shaking flasks at 28 °C, 175 rpm for 3 days. The G1 yeast cells were harvested by centrifugation of the cell biomass at 2711 xg for 5 min, and the precipitated cell pellet was washed once with Milli-Q water, lyophilized, and stored at room temperature until used. Fungal pellets were formed by

growing the filamentous fungus strain *P. chrysogenum* H3 using the protocol developed by

Moreno-García et al.[27]. Briefly, the fungus was pre-grown in a sporulation medium

containing 1.7 wt./vol.% corn meal agar, 0.1 wt./vol.% yeast extract, 0.2 wt./vol.% glucose

and 2 wt./vol.% agar for 7 days at 28 °C. Yeast nitrogen base medium without amino acids,

containing 0.5% gluconic acid as a carbon source and buffered to pH 7 with Na_2HPO_4 and

KH_2HPO_4, was used as the growth medium for fungal pellet formation. 50 mL of the

medium in a 250 mL flask was inoculated with $4*10^6$ *P. chrysogenum* H3 spores and shaken

at 28 °C, 175 rpm for 6 days. Under these culture conditions, spherical fungal pellets with

diameters of approx. 5 to 8 mm were formed. The harvested fungal pellets were washed in

Milli-Q water, lyophilized, and stored at room temperature until used.

2.3. Vacuum-facilitated infusion of curcumin in single-cell and multicellular encapsulation systems

Three encapsulation systems were developed in the current study for curcumin, the model

compound: the single-cell system using *S. cerevisiae* G1 yeast cells as the carrier (YE-c), the

multicellular systems using fungal pellet as the encapsulation matrices (FP-c), and the

combination of these two systems (YE/FP-c). For YE-c and FP-c, curcumin was infused into

the G1 yeast cells as described in a previous study [29]. Briefly, before encapsulation, the

freeze-dried, heat inactivated G1 yeast cells were rehydrated and ~ 1g was weighed into a 50

mL centrifuge tube. 3.25 mL of milli-Q water, 1.5 mL of absolute ethanol, and 250 μL of 2.5

mg/mL curcumin dissolved in absolute ethanol were added to achieve a final ethanol

concentration of 35%, and 0.0625 wt.% curcumin to yeast ratio (on wet basis). For FP-c, ~20

mg of freeze-dried H3 fungal pellets were added to the same concentration of curcumin

ethanolic solution as described for the yeast cells. The samples were subjected to 99%

vacuum with a hold time for 5 seconds. After vacuum infusion, the YE-c samples were centrifuged at 2711 xg for 5 min, and the supernatant was decanted. The pelleted cells were then washed 4 times in 5 mL of milli-Q water and centrifuged once more to remove excess water. The FP-c samples were separated from the curcumin solution and stirred in milli-Q water for 5 min, then blotted dry to remove excess water. To prepare YE/FP-c, YE-c and H3 fungal pellets were mixed at dry mass ratio of 3:1 in water, then subjected to the same vacuum treatment and washing protocol as FP-c samples. A patent application [application number: 64/411,843] has shown that yeast cells could be efficiently immobilized in fungal biomass using this vacuum procedure. Overall, in this study vacuum facilitated infusion has two key roles- first is the infusion of the small molecules in cell-based carriers including multicellular fungal pellet system and second is the enhanced permeation of yeast cells in fungal pellet. The proposed working principle for the vacuum infusion of the small molecules is based on enhanced rate of partitioning of curcumin into cells facilitated by the removal of ethanol from the aqueous solution. Vacuum facilitated permeation of yeast cells in fungal pellets is enabled by the infusion of liquid upon removal of air pockets from the porous fungal pellet matrix. The yeast cells suspended in the liquid are infused into the porous fungal pellet with the liquid. This process has also been used for the infusion of bacterial cells in plant tissues [30]. To quantify the encapsulation yield, curcumin was extracted from the encapsulation systems using pure DMSO. The concentration of extracted curcumin was quantified based on the absorbance at 434 nm with a UV-Vis spectrophotometer (GENESYS 10S Series, Thermo Scientific) after appropriate dilution. The concentration of curcumin in the extractant was calculated using a reference calibration curve. Encapsulation yield was calculated as the amount of curcumin per unit dry mass of the encapsulation matrices.

2.4. Microscopic imaging of the multicellular encapsulation systems

2.4.1. Scanning electron microscope

To analyze the microstructure of fungal pellets, the outer and inner surface of the pellets were imaged using a Thermo Fisher Quattro S Environmental scanning electron microscope (SEM) (Thermo Scientific, Rochester, NY, USA) in a high vacuum mode using 5 kV accelerating voltage for locating and focusing on the specimen before a brief increase to 15 kV for imaging. Prior to SEM imaging, fungal pellets with or without immobilized G1 yeast cells were freeze-dried and gold-sputter-coated. To observe the inner area of the fungal pellets, pellets were cut in half with a scalpel.

2.4.2. Fluorescence microscopic imaging

Fungal pellets were sliced and stained with fluorescent dyes before imaging. To facilitate slicing, each fungal pellet was submerged in 1.5% warm agarose and cooled until solid. The piece of agarose containing the fungal pellet was cut out and mounted on the slicing platform of an oscillating tissue slicer (OTS-4500, Electron Microscopy Sciences, Hatfield, PA, USA). 250 μm thick specimens were obtained and transferred to glass slides. Calcofluor white (CFW) and Nile red (NR) were used to stain the cell wall and intracellular lipid of the fungal hyphae cells, respectively. Approximately 300 μL of CFW (10 $\mu g/mL$) and NR (5 $\mu g/mL$) solution were deposited on the fungal pellet specimen and incubated for 15 min before rinsing with water. A Leica TCS SP8 Multiphoton microscope (Leica Microsystem Inc.) equipped with a Mai Tai DeepSee laser was used for imaging the specimens. A 710 nm laser excitation wavelength and 426- 506 nm emission filter were used for imaging the fluorescence signal from CFW;

925 nm excitation and 592 - 644 nm emission filters were used for imaging the fluorescence signal from NR.

The autofluorescence of curcumin was utilized to visualize the encapsulated curcumin in the encapsulation matrices. Due to the significant signal overlap between CFW and curcumin, Congo red (1 mg/mL) was used to stain the cell wall instead [31]. The excitation and emission wavelengths for curcumin were set to 760 nm, 475- 575 nm; and those for Congo red were set to 910 nm, 592 - 644 nm.

2.5. Release of curcumin from the encapsulation systems during *in vitro* digestion

2.5.1. Release kinetics

Simulated gastric and small intestinal fluid were prepared according to the protocol developed by Minekus et al. [32] with some modifications. When preparing the electrolyte stock solutions for the digestion fluids, $NaHCO_3$ was replaced with equal molarity of NaCl and $(NH_4)_2CO_3$ was replaced with $(NH_4)_2SO_4$ to avoid a change of pH during storage. Immediately before use, 2.5 mg/mL pepsin was added to the simulated gastric fluid (SGF), and the pH was adjusted to pH 3; 10 mg/mL pancreatin and 5 mg/mL bile salts were added to the simulated small intestinal fluid (SIF) and the pH was adjusted to 7. Approximately 15 mg (dry mass) of YE-c, or 6 pellets of FP-c / YE/FP-c were weighed into 50 mL centrifuge tubes. 5 mL of SGF pre-warmed to 37 °C was added to each tube and vortexed to suspend the cells. The sample-to-digestion fluid ratios were determined to guarantee a sink condition for curcumin while also ensuring that the concentration of curcumin in the supernatant would be above the detection limit for all samples at all time points. SGF was sampled at 60 and 120 min and centrifuged to remove any insoluble solids. The concentration of curcumin in SGF was evaluated by

measuring the absorbance of the supernatant using the UV-VIS spectrophotometer at 424 nm. After 2 hours, the samples were harvested from SGF and transferred to the same volume of pre-warmed SIF. Then, the SIF was sampled and measured for absorbance at 30, 60, 90, 120, 150, and 180 min in the same manner. The concentration of curcumin released to the supernatant was calculated according to established calibration curves. At the end of the simulated digestion, retained curcumin in the encapsulation matrices was extracted using DMSO and quantified as specified in Section 2.2. Cumulative release of curcumin at each time point during the gastric and intestinal phases was calculated from the measurements.

The cumulative release fraction of curcumin from the three encapsulation systems in SIF (Equation 1) was fitted to an empirical Weibull model (Equation 2), proposed by Langenbucher [33] to describe drug release curves.

$$M_t = \frac{m_{SIF}^t}{m_{tot.} - m_{SGF}}$$

<div align="right">*Equation 1*</div>

$$M_t = 1 - exp\left(-\left(\frac{t}{\gamma}\right)^k\right)$$

<div align="right">*Equation 2*</div>

M_t is the cumulative release fraction of curcumin during the small intestinal phase at time t (min); m_{SIF}^t is the amount (μg) of curcumin released into SIF at time t; m_{tot} and m_{SGF} are the total loading of curcumin in the encapsulation system and total amount released during the gastric phase. γ (min), and k (dimensionless) are the scale and shape parameters of the Weibull model. The goodness of curve fitting was assessed by the root mean squared error (RMSE) and the correlation coefficients between true and fitted values.

2.5.2. Fluorescence microscopic characterization

FP-c and YE/FP-c samples were collected before digestion, after the gastric phase, and after the small intestinal phase to visualize the changes in the spatial distribution of curcumin within the multicellular encapsulation systems during *in vitro* digestion. The samples were sliced, stained with Congo red, and imaged with the multiphoton microscope as specified in Section 2.3.2.

2.6. Statistical analysis

All experiments were conducted in triplicate, and each batch of samples was analyzed as described above. Pairwise t-tests were conducted to compare the means among the three encapsulation systems for the encapsulation yield. Repeated measures ANOVA was used to compare gastric phase release of curcumin across time points and encapsulation systems. P-values smaller than 0.05 were considered statistically significant.

3. Results and discussion

3.1. Microstructure of the multicellular encapsulation systems

The spherical fungal pellets formed by *P. chrysogenum* H3 showed typical features of a filamentous fungus biomass grown under submerged shaking conditions: an intertwined hyphae matrix with a hollow or sparse interior core. The H3 fungal pellets had a dense layer of hyphae near the surface, and sparser distribution of hyphae towards the core, as illustrated by the SEM images of the outer surface and the interior section of a pellet and the fluorescence microscopic image of the pellet cross-section (**Figure 1**). Such an observation was consistent with the previous reports of fungal pellets formed by *P. chrysogenum* H3 and other filamentous fungi [14,22,34]. With the pre-formed fungal pellets and pre-grown *S. cerevisiae* G1 yeast cells, curcumin was encapsulated using vacuum-facilitated infusion,

resulting in the two encapsulation systems: FP-c and YE-c. Subsequently, YE/FP-c was created by immobilizing curcumin-loaded G1 yeast cells (YE-c) in the pre-formed H3 fungal pellet through a rapid internalization facilitated by the vacuum treatment. The results based on fluorescence microscopy and SEM images (**Figure 2)** demonstrate that after the vacuum treatment, yeast cells were present at both the surface and core of the fungal pellets. The SEM images (Figure 2A) showed that more yeast cells were present near the core than at the outer surface. The fungal pellet's outer surface contained hyphae protruding from the pellet, and this "hairy" layer was less dense than the layer right beneath the surface, where the hyphae formed a more structured intertwined network. Moreover, after vacuum treatment to enable immobilization of yeast cells, the fungal pellets were immediately rinsed with water, thus the loosely attached yeast cells near the outer surface of the fungal pellet were washed away, while those physically trapped in the hyphae network were retained, resulting in the observed distribution of yeast cells as indicated by the SEM images in Figure 2.

3.2. Infusion of curcumin in the encapsulation systems

The two multicellular encapsulation systems (FP-c and YE/FP-c) were prepared by directly infusing curcumin into the fungal pellet or infusing into G1 yeast cells first, which were then immobilized with the fungal pellet. **Figure 3** shows the location of curcumin within the two encapsulation systems after vacuum infusion. Curcumin was internalized into either H3 fungal hyphae cells or G1 yeast cells. In the YE/FP-c system, the majority of curcumin was encapsulated in G1 cells, while limited amounts of curcumin could be seen inside the fungal hyphae cells as there could be some unencapsulated curcumin that partitioned into the hyphae cells during vacuum facilitated internalization of G1 cells into the fungal pellets. **Table 1** summarizes the encapsulation yield of curcumin in the three

encapsulation systems, expressed on a dry mass basis. YE-c and FP-c had similar

encapsulation yields (3.13±0.01 and 3.52±0.40 mg/g, p-value>0.05), which were

significantly higher than that in YE/FP-c (0.87±0.02 mg/g). Young et al [29] used the same

vacuum infusion method to encapsulate curcumin into single yeast cells and reported a

similar encapsulation yield as the results in the current study. A higher encapsulation yield of

curcumin in yeast cells has been reported by Paramera et al.[5,35] In their studies, a much

higher compound-to-cell ratio was used, which could result in a higher encapsulation yield.

Furthermore, in their study, curcumin was dispersed in water or ethanolic solution at a

concentration higher than the solubility of curcumin in corresponding solvents. Thus, the

potential presence of un-dissolved curcumin crystals in the yeast cell suspension could

influence the reported yield in the previous study as these crystals may not be removed

during washing. To the authors' knowledge, no previous study has evaluated the

encapsulation yield of curcumin into filamentous fungal cells. The results of the current study

(**Table 1**) imply that under the current compound infusion conditions, similar encapsulation

yields were achieved using different cell types (G1 yeast cells vs. H3 fungal cells). The

amount of curcumin in the YE/FP-c system was limited by the number of YE-c cells that

could be immobilized in the fungal pellets, since in this system, curcumin was only loaded

into G1 yeast, not directly in FP. With a similar encapsulation efficiency of curcumin in

single G1 yeast cells and H3 fungal cells, we could conclude that the encapsulation yield of

curcumin in YE/FP-c to some extent reflects the mass fraction of G1 yeast cells immobilized

in the multicellular FP. The vacuum-facilitated method has been shown to immobilize 6

times more yeast cells inside *Aspergillus oryzae* 76-2 fungal pellet compared to the

traditional co-incubation method (data not shown).

3.3. Release kinetics of curcumin from the encapsulation systems during *in vitro* digestion

The release profile of curcumin was evaluated for the three encapsulation systems using an *in vitro* static digestion model. The *in vitro* digestion included 2 hours of gastric phase followed by a 3-hours small intestinal phase. Consistent with results reported in previous studies about yeast-based microcarriers for curcumin [36], limited release of curcumin was observed during the gastric phase: 13±2%, 21±4%, and 30±14% for YE/FP-c, FP-c, and YE-c respectively at the end of 2 hours (**Figure 4A**). Based on the repeated measures ANOVA result, the curcumin release percentage during the gastric phase was not significantly different across time points or different encapsulation systems. The three encapsulation systems showed different kinetic profiles of curcumin release during the 3-hour small intestinal phase (**Figure 4B**). During the small intestinal digestion phase, the cumulative percentage of release was highest from YE-c (82.9%), followed by FP-c (45.7%), and lowest from YE/FP-c (29.2%). The rapid initial release was observed in both the YE-c and YE/FP-c systems. For YE-c, 71.1% of curcumin retained after the gastric phase was released within the first 30 min of the small intestinal phase, while around 10% was released in the subsequent 2.5 hours. For YE/FP-c, 18.6% was released within 30 min and an additional 14.7% in the following 2.5 hours. Different from these two systems, curcumin was gradually released from FP-c without initial rapid release. The difference in release kinetics of the three encapsulation systems was captured by the fitting parameters of the Weibull model (Equation 2). Many mathematical models have been proposed to describe the drug release kinetics, such as zeroth order, first order, Higuchi, Peppas, Weibull model etc. [37]. Among these models, the Weibull model has significant flexibility in modeling diverse shape factors and

release time scales using a two-parameter equation and was selected for the quantitative comparison of these release profiles. The selected model fits all three release kinetic curves well, as indicated by the low RMSE and high correlation coefficients (**Table 2**). The scale parameter (γ) defines the timescale of the curcumin release process, which is in an increasing order of YE-c < FP-c < YE/FP-c, indicating that the overall release rate was fastest for the YE-c and slowest for the YE/FP-c. The shape parameter (k) reflects the types of curves: k<1 indicates a parabolic curve with a large initial slope and a consistent exponential character; k=1 simplifies the model to an exponential distribution; k>1 indicates a sigmoidal curve with ascending curvature delimited by an inflection point [37]. YE-c and YE/FP-c had k<1, consistent with the observation of rapid initial release from these two systems. FP-c had the fitted k value very close to 1, demonstrating a nearly exponential release behavior.

Comparing the release of curcumin from YE/FP-c to that from YE-c and FP-c (**Figure 4B**), we could decouple the cell carrier effect and the matrix effect endowed by the filamentous fungus. In FP-c, the fungal cells served as both the carriers for curcumin and the 3D matrix itself, whereas for YE/FP-c, the carriers for curcumin were the G1 yeast cells and the fungal hyphae network was only used as a 3D matrix. The release of curcumin from G1 yeast cells (YE-c) showed the same pattern as in other single yeast cell-based encapsulation systems [5,36]. The multicellular encapsulation systems, FP-c and YE/FP-c, modified the release profile of curcumin compared to the single-yeast system from two aspects: it eliminated or reduced the initial rapid release and reduced the overall release rate of curcumin. The rapid release in the single cell encapsulation system results from the interactions of bile salts with the cells and the associated release of encapsulated curcumin as discussed in the results of our previous study [36]. In addition to the influence of bile salts, the

gastric digestion phase also contributes to preconditioning of the cells to facilitate release of encapsulated bioactives [36]. In the case of YE/FP-c, the initial rapid release is potentially due to the interactions of bile salts with encapsulated curcumin in yeast cells near the surface of fungal pellet. It is likely that the fraction of the yeast cells near the surface of fungal pellet can rapidly interact with bile salts and resulting in a rapid release of a small fraction of curcumin. This trend of rapid release was not observed for FP-c. Thus, reflecting the role of the fungal matrix in modulating the interactions of bile salts and encapsulated curcumin. Potential factors modulating the release of curcumin in fungal pellet were further investigated using fluorescence microscopy as discussed in the next section.

3.4. Microscopic characterization of the multicellular encapsulation systems during *in vitro* digestion

Fluorescence microscopic imaging was used to visualize the spatial and temporal changes in the distribution of curcumin in fungal pellet during digestion. **Figure 5** shows the distribution of curcumin in the multicellular encapsulation systems before digestion, after the gastric phase, and after the small intestinal phase. The hyphae cell wall was stained with Congo red to visualize the fungal biomass [31]. After the gastric phase, there was no significant change in the curcumin distribution in the multicellular matrices compared to the control samples before digestion. Curcumin mainly remained within either fungal hyphae cells or G1 yeast cells in the FP-c and YE/FP-c systems, respectively. After the intestinal phase, however, a band of residual curcumin-rich aggregates was observed to localize just beneath the surface of the fungal pellets in both systems, while no significant amount of curcumin was retained inside the cells where it was originally encapsulated. Such a phenomenon was observed for both FP-c and YE/FP-c. Images were taken at a higher magnification at the

surface and core of YE/FP-c after the small intestinal phase (**Figure S1**). The G1 yeast cells inside the fungal pellet remained immobilized after the *in vitro* digestion process, while the encapsulated curcumin was released from the cells and migrated outwards from the core. Furthermore, some of the released curcumin was deposited near the surface of the fungal pellet. The close-up images show that the curcumin-rich band near the pellet surface was not G1 yeast cells carrying curcumin but some form of curcumin aggregates. To further elucidate the composition of these aggregates, Nile Red was used to stain the neutral lipid in the native fungal pellet and the FP-c sample after the small intestinal digestion phase. The colocalization of fluorescence signals of curcumin and Nile Red in the post-digestion FP-c sample (**Figure 6 A1**, **A2**) suggests that the curcumin aggregates observed near the surface of the fungal pellet after digestion included lipid-rich deposits at the surface along with residual curcumin. **Figures 6B** and **6C** demonstrate that in native fungal pellet without curcumin, such lipid aggregates also appeared near the pellet surface after the small intestinal digestion, confirming the hypothesis that these lipid aggregates were likely extracted from the fungal biomass during digestion facilitated by the lipase and bile salt in SIF [38,39], and deposited beneath the outer surface of the fungal pellet with the highest hyphae density.

Together, the imaging and release kinetics results suggest that the release profile of curcumin in fungal pellets was modulated by the structural and compositional features of the encapsulation matrix. The structural and compositional features of fungal pellets results in the accumulation of curcumin beneath the fungal pellet surface and significantly influences the release of curcumin from fungal pellets. Since the curcumin concentration was approximately constant close to the surface of fungal pellets, the rate of release of curcumin

from fungal pellets was constant and represented a zero-order linear release process (**Table S1**).

In our previous work [7], we studied the structural effect of cell clusters on the release of curcumin, where the cell clusters were formed by modifying yeast cell surface with oppositely charged polyelectrolytes coating and subsequent electrostatic aggregation. The cell clustering did mitigate the initial rapid release of curcumin compared to single cells, but such an effect diminished after 1 hour of the small intestinal phase, and the cumulative release at the end was similar for single cells and multi-cell clusters. Unlike the multicellular systems in the current study, the cell clusters were smaller in dimension (50 - 100 μm), loosely bounded, and irregularly shaped, also they did not possess a well-defined surface with the densely intertwining outer wall. Thus, the structural or matrix effect provided by these cell clusters was limited. In contrast, the influence of multicellular organization of fungal cells and their hyphae in filamentous fungal pellets on release characteristics was much more prominent, as indicated by the differences in the release kinetics of single cells compared to fungal pellet encapsulation systems (**Table 2**). A similar influence of natural multicellular organization on the release of micronutrients during simulated digestion has been reported for other plant tissues. For example, a study has illustrated the release of intracellular nutrients from the surface cells of cut almond seed cubes corresponding to the ruptured cell walls, and gradually, the release was extended to the inner intact cells over a period of 12 hours[36]. Palmero et al.[37] also reported that the bioaccessibility of β-carotene in orange carrots was lower in large cell clusters (800 - 2000 μm) than in small cell clusters (40-250 μm).

4. Conclusion

In summary, the results of this study demonstrate development of multi-cellular encapsulation systems using a low energy vacuum infusion process with sustainable fungal based biomaterials and compare the results with a single cell encapsulation system. The unique advantages of the cell-based encapsulation systems compared to emulsions in improving loading yield, and oxidative and thermal stability has been discussed in previous studies [6,40]. The current study illustrates that the vacuum infusion process can provide efficient encapsulation of bioactives in a multicellular system with a uniform loading across multiple cell layers of cells. The results also illustrate that the multi-cellular system using fungal pellets had a lower rate of release of encapsulated model bioactive as compared to the single cell model system. This result is significant as modulation of release characteristics can be a potential approach to achieve delivery of bioactives across different sections of the gut including the large intestine. In addition, the results of this study also illustrate the potential barriers in multi-cellular systems for the release of bioactives compared to single cells. The results of this study also have potential implications for the release of bioactives from multicellular plant and animal tissues and application of fungal biomaterials as alternative protein products.

5. Conflicts of interest

There are no conflicts of interest to declare.

6. Acknowledgment

(MYA-2451) strain and the filamentous fungus strain *Penicillium chrysogenum* H3 (UCDFST 22-

448) were kindly provided by the Department of Microbiology at University of Cordoba, Spain.

Tables

Table 1: Encapsulation yield of curcumin in YE-c, FP-c, and YE/FP-c.

Encapsulation system	Encapsulation yield (mg/g d.b.*) (mean±sd, n=3)
YE-c	3.13±0.01[a]
FP-c	3.52±0.40[a]
YE/FP-c	0.87±0.02[b]

* d.b.: dry mass basis.

Table 2: Weibull model parameters fitted to the release of curcumin from the yeast-based encapsulation systems during *in vitro* small intestinal digestion, plus the model fitting RMSE and correlation coefficients.

Encapsulation system	Scale (γ)	Shape (k)	RMSE	Correlation
YE-c	23.78	0.17	0.043	0.996
FP-c	265.18	1.13	0.015	0.986
YE/FP-c	2426.38	0.36	0.009	0.996

Figure captions (Figures also submitted as separate files)

A.

Pellet inner surface
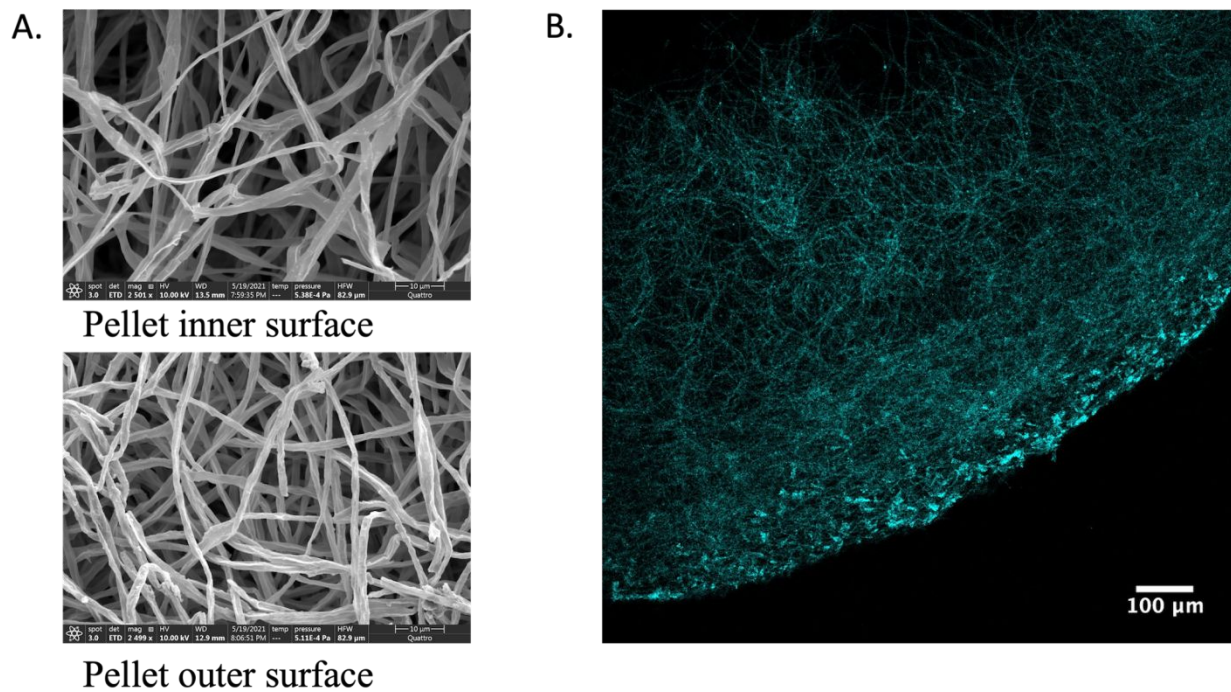
Pellet outer surface

B.

100 µm

Figure 1: Characteristic images of Penicillium chrysogenum H3 fungal pellet. (A) SEM (scale bar=10 µm)*, (B) Multiphoton fluorescence microscope (stained with calcofluor white)* (scale bar=100 µm)*.*
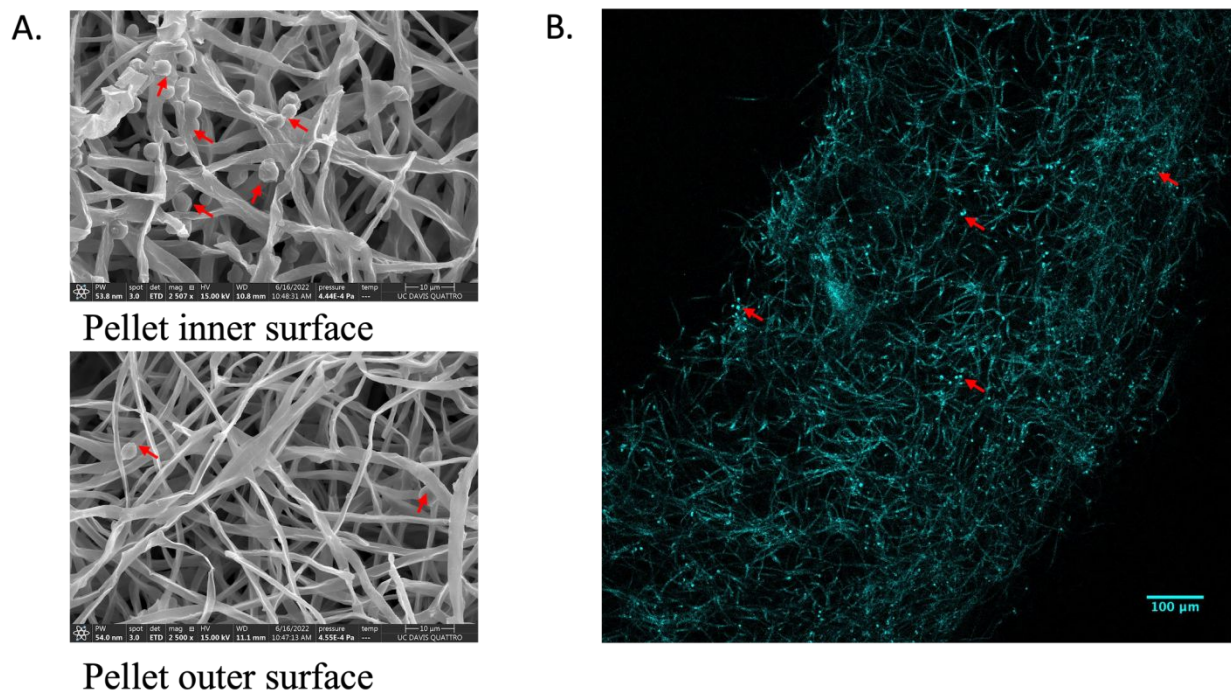
A.

Pellet inner surface

Pellet outer surface

B.

100 µm

Figure 2: Characteristic images of S. cerevisiae G1 cells infused in P. chrysogenum H3 fungal pellet. (A) SEM (scale bar=10 μm), (B) Multiphoton fluorescence microscope (stained with calcofluor white) (scale bar=100 μm). The red arrows point to some of the G1 yeast cells in the images.
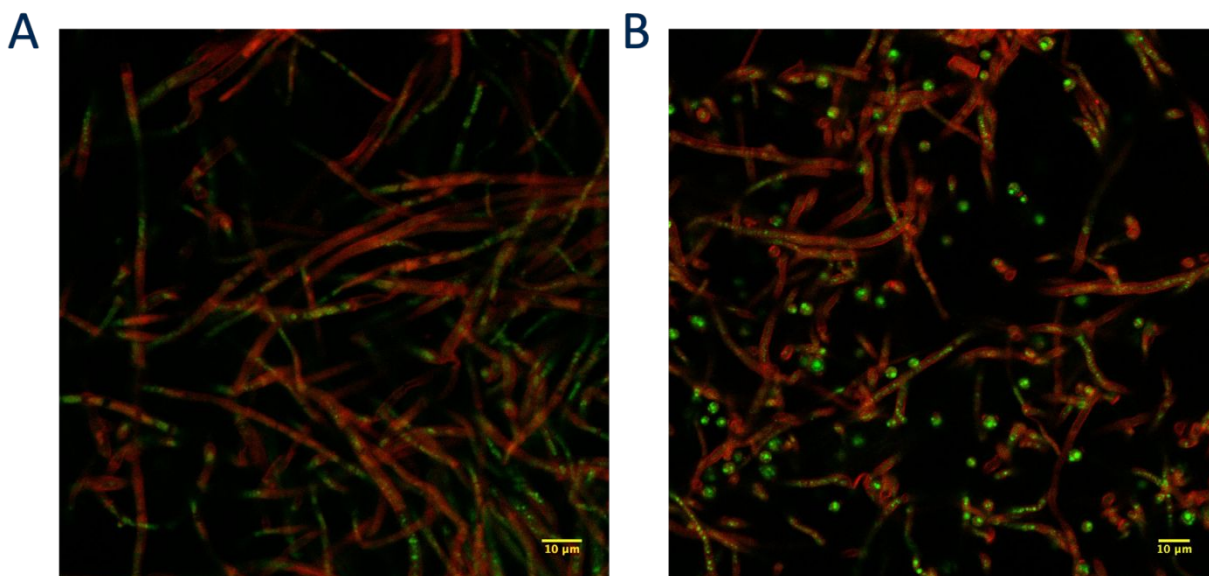

Figure 3: Multiphoton fluorescence images of FP-c (A) and YE/FP-c (B) showing the localization of curcumin (green) in the fungal pellet (fungal hyphae cell walls were stained with Congo red) (scale bar=10 μm).
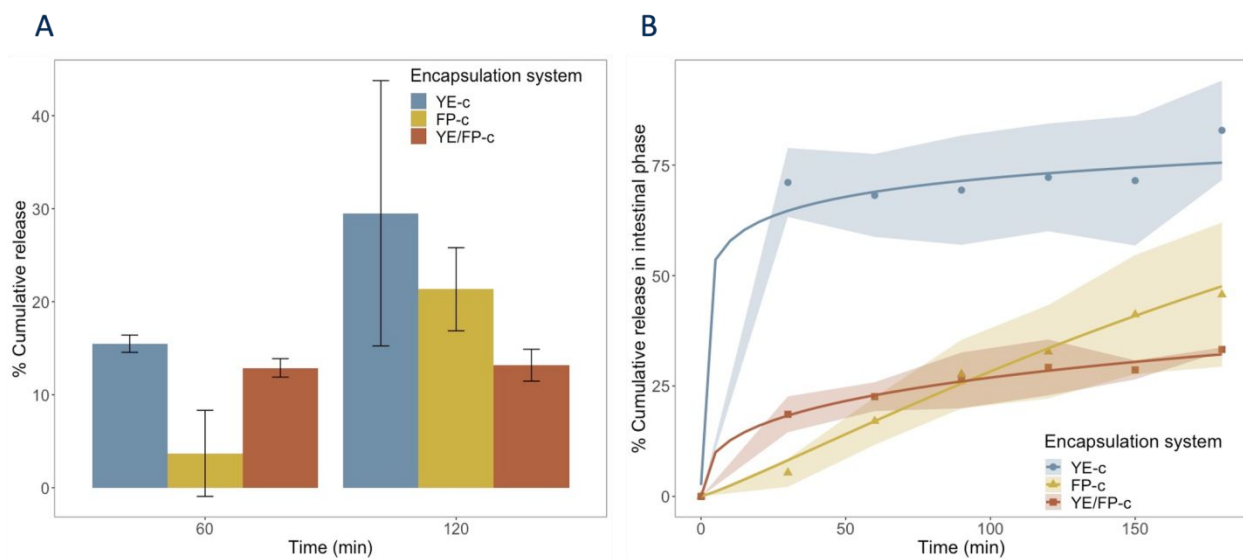

Figure 4: In vitro release of curcumin from three encapsulation systems during simulated digestion. **(A) 2-hour gastric phase.** The bar height and error bars indicate the mean and standard deviation (n=3) of the % cumulative release of each encapsulation system at each time point. *(B) 3-hour small intestinal phase.* The markers are the mean % cumulative release (n=3). The banded areas represent the pointwise 95% confidence interval. The solid lines are the fitted Weibull model for each encapsulation system.
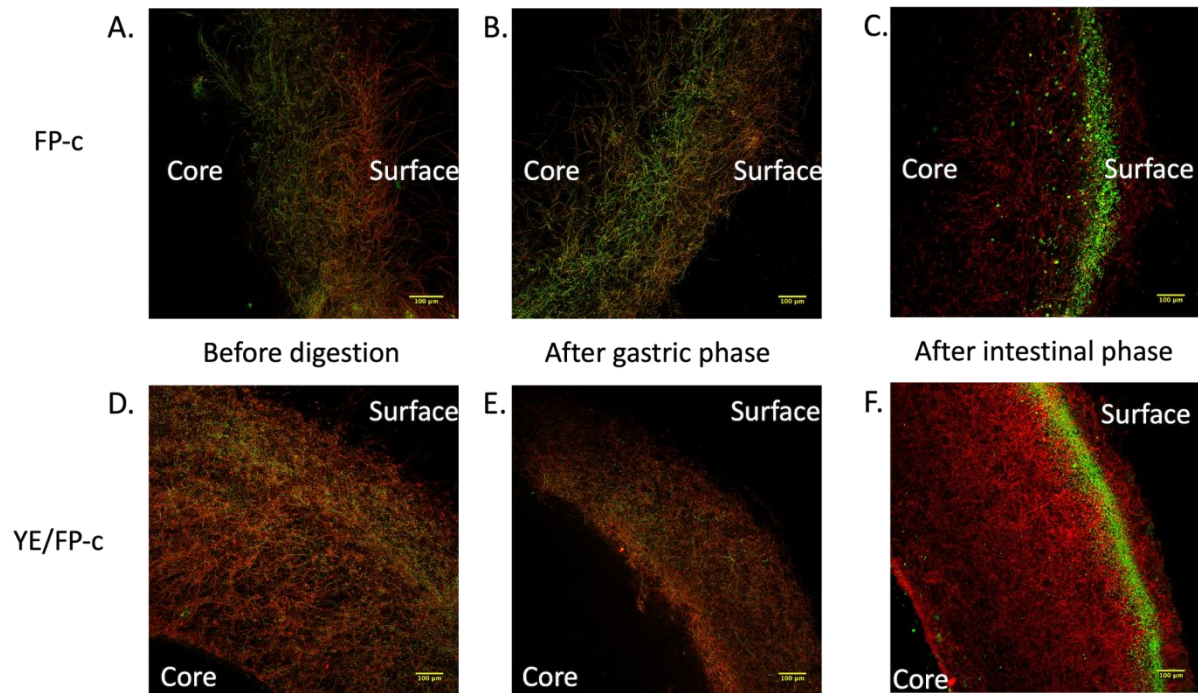
Figure 5: Multiphoton fluorescence microscopic images showing the change in curcumin (green) ***distribution in the two multicellular encapsulation systems: FP-c (A-C) and YE/FP-c (D-F)*** (fungal hyphae cell wall stained by Congo red) ***before digestion (A,D), after the gastric phase (B,E), and after the small intestinal phase (C,F)*** (scale bar=100 *μm*)*.*
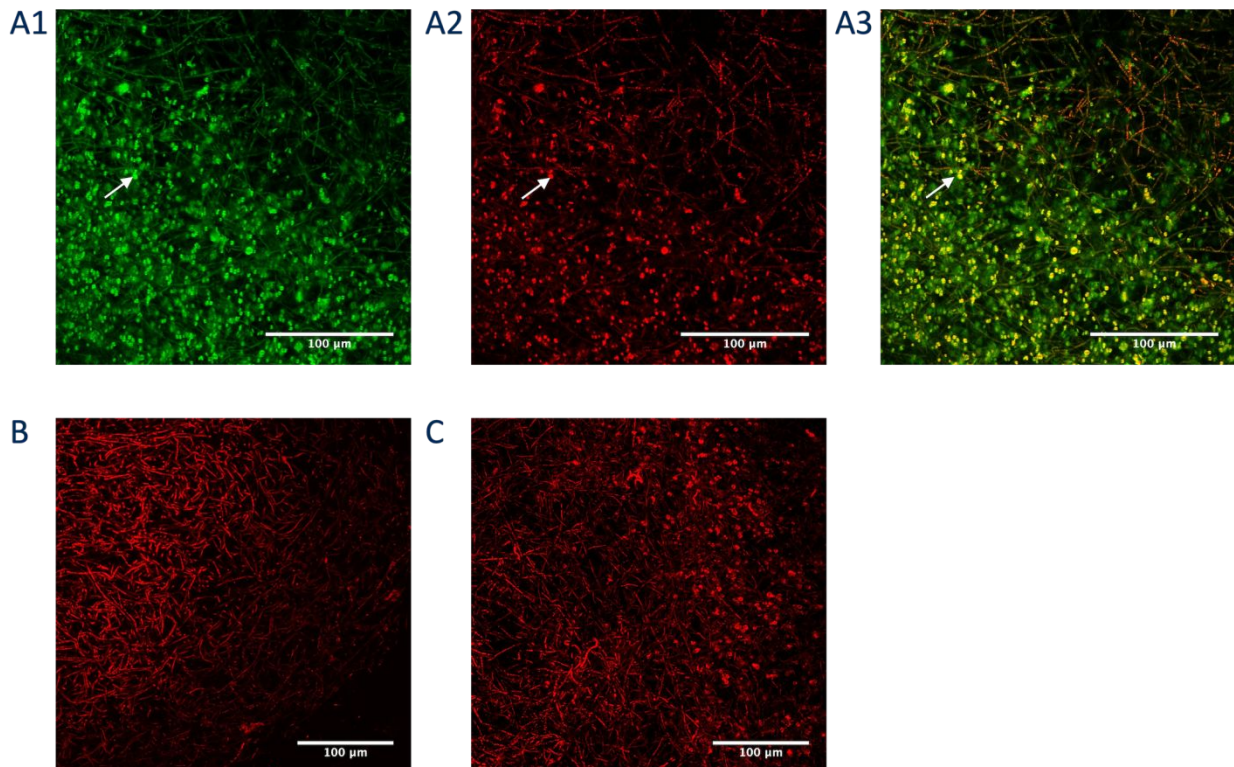
Figure 6: Multiphoton microscopic images of the post-digestion FP-c near the fungal pellet surface: curcumin channel (A1), Nile Red channel (A2); composite of the two channels (A3); Nile red-stained native fungal pellet before (B) and after digestion (C). Scale bar = 100 μm. The white arrows point to one of the lipid-rich aggregates observed in post-digestion fungal pellet samples.

Bibliography

1.   J. E. Aguilar-Toalá, D. Quintanar-Guerrero, A. M. Liceaga and M. L. Zambrano-Zaragoza, Encapsulation of bioactive peptides: a strategy to improve the stability, protect the nutraceutical bioactivity and support their food applications., *RSC Adv.*, 2022, **12**, 6449–6458.

2.   J. Luana Carvalho de Queiroz, I. Medeiros, A. Costa Trajano, G. Piuvezam, A. Clara de França Nunes, T. Souza Passos and A. Heloneida de Araújo Morais, Encapsulation techniques perfect the antioxidant action of carotenoids: A systematic review of how this effect is promoted., *Food Chem.*, 2022, **385**, 132593.

3.   J. Ubbink and J. Krüger, Physical approaches for the delivery of active ingredients in foods, *Trends Food Sci. Technol.*, 2006, **17**, 244–254.

4.   G. Shi, L. Rao, H. Yu, H. Xiang, G. Pen, S. Long and C. Yang, Yeast-cell-based microencapsulation of chlorogenic acid as a water-soluble antioxidant, *J. Food Eng.*, 2007, **80**, 1060–1067.

5.   E. I. Paramera, S. J. Konteles and V. T. Karathanos, Stability and release properties of curcumin encapsulated in Saccharomyces cerevisiae, β-cyclodextrin and modified starch, *Food Chem.*, 2011, **125**, 913–922.

6.   S. Young and N. Nitin, Thermal and oxidative stability of curcumin encapsulated in yeast microcarriers., *Food Chem.*, 2019, **275**, 1–7.

7.   K. Feng, Y. Wei, T. Hu, R. J. Linhardt, M. Zong and H. Wu, Colon-targeted delivery systems for nutraceuticals: A review of current vehicles, evaluation methods and future prospects, *Trends Food Sci. Technol.*, 2020, **102**, 203–222.

8.   Y. Lu, R. Rai and N. Nitin, Engineering cell-based microstructures to study the effect of structural complexity on in vitro bioaccessibility of a lipophilic bioactive compound., *Food Funct.*, 2022, **13**, 6560–6573.

9.   J. P. Blakeman, A. R. McCracken and D. A. Seaby, Changes brought about in solid substrates after fermentations of mixtures of cereals and pulses withRhizopus oryzae, *J. Sci. Food Agric.*, 1988, **45**, 109–118.

10.   R. Gmoser, R. Fristedt, K. Larsson, I. Undeland, M. J. Taherzadeh and P. R. Lennartsson, From stale bread and brewers spent grain to a new food source using edible filamentous fungi., *Bioengineered*, 2020, **11**, 582–598.

11.   Seyedeh Fatemeh Seyed Reihani and K. Khosravi-Darani, Mycoprotein Production from Date Waste Using Fusarium venenatum in a Submerged Culture, *Applied Food Biotechnology*, 2018.

12.   P. F. Souza Filho, D. Andersson, J. A. Ferreira and M. J. Taherzadeh, Mycoprotein: environmental impact and health aspects., *World J. Microbiol. Biotechnol.*, 2019, **35**, 147.

13.   P. A. Gibbs, R. J. Seviour and F. Schmid, Growth of filamentous fungi in submerged culture: problems and possible solutions., *Crit. Rev. Biotechnol.*, 2000, **20**, 17–48.

14.   J. Zhang and J. Zhang, The filamentous fungal pellet and forces driving its formation., *Crit. Rev. Biotechnol.*, 2016, **36**, 1066–1077.

15.   A. Amanullah, P. Jüsten, A. Davies, G. C. Paul, A. W. Nienow and C. R. Thomas, Agitation induced mycelial fragmentation of Aspergillus oryzae and Penicillium chrysogenum., *Biochem. Eng. J.*, 2000, **5**, 109–114.

16.   H. Y. Makagiansar, P. Ayazi Shamlou, C. R. Thomas and M. D. Lilly, The influence of mechanical forces on the morphology and penicillin production of Penicillium chrysogenum, *Bioprocess Engineering*, 1993, **9**, 83–90.

17.   M. Ogawa, L. F. Bisson, T. García-Martínez, J. C. Mauricio and J. Moreno-García, New insights on yeast and filamentous fungus adhesion in a natural co-immobilization system: proposed advances and applications in wine industry., *Appl. Microbiol. Biotechnol.*, 2019, **103**, 4723–4731.

18.   N. Mohd Nasir, F. H. Mohd Yunos, H. H. Wan Jusoh, A. Mohammad, S. S. Lam and A. Jusoh, Subtopic: Advances in water and wastewater treatment harvesting of Chlorella sp. microalgae using Aspergillus niger as bio-flocculant for aquaculture wastewater treatment., *J. Environ. Manage.*, 2019, **249**, 109373.

19.   W. Zhou, Y. Cheng, Y. Li, Y. Wan, Y. Liu, X. Lin and R. Ruan, Novel fungal pelletization-assisted technology for algae harvesting and wastewater treatment., *Appl. Biochem. Biotechnol.*, 2012, **167**, 214–228.

20.   A. F. Miranda, M. Taha, D. Wrede, P. Morrison, A. S. Ball, T. Stevenson and A. Mouradov, Lipid production in association of filamentous fungi with genetically modified cyanobacterial cells., *Biotechnol. Biofuels*, 2015, **8**, 179.

21.   A. Bhattacharya, M. Mathur, P. Kumar and A. Malik, Potential role of N-acetyl glucosamine in Aspergillus fumigatus-assisted Chlorella pyrenoidosa harvesting., *Biotechnol. Biofuels*, 2019, **12**, 178.

22.   M. Ogawa, J. Moreno García, N. Nitin, K. Baar and D. E. Block, Assessing edible filamentous fungal carriers as cell supports for growth of yeast and cultivated meat, *Foods*, 2022, **11**, 3142.

23.   T. García-Martínez, A. Puig-Pujol, R. A. Peinado, J. Moreno and J. C. Mauricio, Potential use of wine yeasts immobilized on Penicillium chrysogenum for ethanol production, *J. Chem. Technol. Biotechnol.*, 2012, **87**, 351–359.

24.   R. A. Peinado, J. J. Moreno, J. M. Villalba, J. A. González-Reyes, J. M. Ortega and J. C. Mauricio, Yeast biocapsules: A new immobilization method and their applications, *Enzyme Microb. Technol.*, 2006, **40**, 79–84.

25.   M. Ogawa, P. Carmona-Jiménez, T. García-Martínez, J. V. Jorrín-Novo, J. Moreno, M. D. Rey and J. Moreno-García, Use of yeast biocapsules as a fungal-based immobilized cell technology for Indian Pale Ale-type beer brewing., *Appl. Microbiol. Biotechnol.*, 2022, **106**, 7615–7625.

26.   J. R. López-Menchero, M. Ogawa, J. C. Mauricio, J. Moreno and J. M. García, Effect of calcium alginate coating on the cell retention and fermentation of a fungus-yeast immobilization system, *LWT*, 2021, 111250.

27.   J. Moreno-García, T. García-Martinez, J. Moreno, J. C. Mauricio, M. Ogawa, P. Luong and L. F. Bisson, Impact of Yeast Flocculation and Biofilm Formation on Yeast-Fungus Coadhesion in a Novel Immobilization System, *Am. J. Enol. Vitic.*, 2018, **69**, 278–288.

28.   P. J. Strong, R. Self, K. Allikian, E. Szewczyk, R. Speight, I. O'Hara and M. D. Harrison, Filamentous fungi for future functional food and feed., *Curr. Opin. Biotechnol.*, 2022, **76**, 102729.

29.   S. Young, S. Dea and N. Nitin, Vacuum facilitated infusion of bioactives into yeast microcarriers: Evaluation of a novel encapsulation approach., *Food Res. Int.*, 2017, **100**, 100–112.

30.   C. W. Simmons, J. S. VanderGheynst and S. K. Upadhyaya, A model of Agrobacterium tumefaciens vacuum infiltration into harvested leaf tissue and subsequent in planta transgene transient expression., *Biotechnol. Bioeng.*, 2009, **102**, 965–970.

31.   M. Slifkin and R. Cumbie, Congo red as a fluorochrome for the rapid detection of fungi., *J. Clin. Microbiol.*, 1988, **26**, 827–830.

32.   M. Minekus, M. Alminger, P. Alvito, S. Ballance, T. Bohn, C. Bourlieu, F. Carrière, R. Boutrou, M. Corredig, D. Dupont, C. Dufour, L. Egger, M. Golding, S. Karakaya, B. Kirkhus, S. Le Feunteun, U. Lesmes, A. Macierzanka, A. Mackie, S. Marze, D. J. McClements, O. Ménard, I. Recio, C. N. Santos, R. P. Singh, G. E. Vegarud, M. S. J. Wickham, W. Weitschies and A. Brodkorb, A standardised static in vitro digestion method suitable for food - an international consensus., *Food Funct.*, 2014, **5**, 1113–1124.

33.   F. Langenbucher, Linearization of dissolution rate curves by the Weibull distribution., *J. Pharm. Pharmacol.*, 1972, **24**, 979–981.

34.   T. García-Martínez, R. A. Peinado, J. Moreno, I. García-García and J. C. Mauricio, Co-culture of Penicillium chrysogenum and Saccharomyces cerevisiae leading to the immobilization of yeast, *J. Chem. Technol. Biotechnol.*, 2011, **86**, 812–817.

35.   E. I. Paramera, S. J. Konteles and V. T. Karathanos, Microencapsulation of curcumin in cells of Saccharomyces cerevisiae, *Food Chem.*, 2011, **125**, 892–902.

36.   S. Young, R. Rai and N. Nitin, Bioaccessibility of curcumin encapsulated in yeast cells and yeast cell wall particles., *Food Chem.*, 2020, **309**, 125700.

37.   Bruschi, in *Strategies to Modify the Drug Release from Pharmaceutical Systems*, Elsevier, 2015, pp. 63–86.

38.   D. Y. Low, B. D'Arcy and M. J. Gidley, Mastication effects on carotenoid bioaccessibility from mango fruit tissue, *Food Res. Int*, 2015, **67**, 238–246.

39.   L. Yonekura and A. Nagao, Intestinal absorption of dietary carotenoids., *Mol. Nutr. Food Res.*, 2007, **51**, 107–115.

40.   A. Czerniak, P. Kubiak, W. Białas and T. Jankowski, Improvement of oxidative stability of menhaden fish oil by microencapsulation within biocapsules formed of yeast cells, *J. Food Eng.*, 2015, **167**, 2–11.